

# A crossed molecular beam study on the reaction of boron atoms, $B(^2P_j)$ , with benzene, $C_6H_6(X^1A_{1g})$ , and D6-benzene $C_6D_6(X^1A_{1g})$

Fangtong Zhang, Ying Guo, Xibin Gu, Ralf I. Kaiser \*

*Department of Chemistry, University of Hawai'i, Honolulu, HI 96822, USA*

Received 2 February 2007; in final form 29 March 2007

Available online 12 April 2007

## Abstract

The reactions of ground-state boron atoms,  $B(^2P_j)$ , with benzene,  $C_6H_6(X^1A_{1g})$ , and deuterated benzene  $C_6D_6(X^1A_{1g})$ , were studied in crossed molecular beam experiments. The reactions were indirect and involved an addition of atomic boron to one carbon atom of benzene following isomerization of the intermediate to the phenylboryl radical,  $C_6H_5BH/C_6D_5BD$ . The latter decomposed via tight exit transition states by cleavage of the *ortho*-carbon–hydrogen/deuterium bonds and concomitant ring closures to the aromatic  $C_6H_5B/C_6D_5B$  isomers, i.e. benzoborirene (**1**), plus atomic hydrogen/deuterium. We also detected the  $^{11}BC_6D_6$  adduct. The derived reaction mechanism is also discussed in light of the isoelectronic  $C_7H_5^+$  surface.

© 2007 Elsevier B.V. All rights reserved.

## 1. Introduction

Considering the potential application of boron as a semi-conductor [1] and as an additive to rocket propellants [2,3], the chemical reactivity of atomic boron,  $B(^2P_j)$ , has attracted considerable attention. Since the boron atom is isoelectronic with singly ionized carbon atoms, an understanding of elementary boron atom reactions can also help to understand the chemistry in weakly ionized hydrocarbon plasmas. Here,  $C^+(^2P_j)$  presents an important reactant in these extreme environments and can contribute, for instance, to the formation of polycyclic aromatic hydrocarbons (PAHs) and their cations [4–6]. Particular interest has been devoted to the synthesis and properties of small hetero-aromatic systems like the cyclic borirene molecule,  $C_2H_3B$  (Fig. 1). In a theoretical study of this molecule in 1962, Voipin has been the first researcher to suggest that trivalent boron portrays the same electronic structure as the carbon cation [7]; this study concluded that the borirene molecule has 70% of the resonance energy of the isoelectronic cyclopropenyl cation [8–10]. In 1987, Eisch et al.

prepared trimesitylborirene and determined its structure via X-ray diffraction [11]. These results suggested that the borirene ring system is aromatic. Finally – in 1997 – Lanzisera et al. successfully isolated the borirene molecule, formed via the reaction of laser ablated boron atoms with ethylene, in an argon matrix [12,13]. The mechanism of its formation was revealed by Balucani et al. by conducting a crossed beam experiment of ground-state boron atoms with ethylene under single collision conditions [14]. Based upon these experimental results, borirene was found to be synthesized via the addition of  $B(^2P_j)$  to the  $\pi$ -bond of the ethylene molecule to form a cyclic borirane radical intermediate. The latter underwent a hydrogen migration from a carbon to the boron atom to yield the borirane radical. Under single collision conditions, this intermediate lost a hydrogen atom to form the aromatic borirene molecule. In a related reaction, Kaiser et al. successfully synthesized a higher-order aromatic molecule, D5-benzoborirene (Fig. 1) in the crossed beam reaction of boron atoms with D6-benzene [15,16]. However, various aspects of this reaction have remained unanswered so far. First, due to our enhanced signal to noise in the present experimental setup, we will investigate if only the atomic hydrogen or also the molecular hydrogen elimination channel is open. Secondly,

\* Corresponding author. Fax: +1 808 956 5908.

E-mail address: [ralfk@hawaii.edu](mailto:ralfk@hawaii.edu) (R.I. Kaiser).

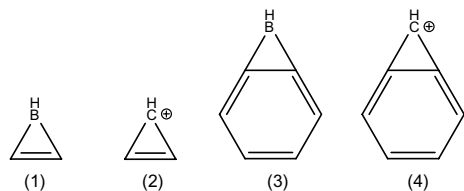


Fig. 1. Schematic structures of the aromatic borirene (1), cyclopropenyl cation (2), benzoborirene (3), and benzocyclopropenyl cation (4).

by conducting the experiment with benzene and D6-benzene at a high signal-to-noise ratio, it will be possible to investigate potential isotope effects and how the reaction mechanism and on the shape of the resulting center-of-mass functions changes. Thirdly, we attempt to detect the hitherto elusive  $^{11}\text{BC}_6\text{H}_6$  and  $^{11}\text{BC}_6\text{D}_6$  adducts. Finally, we will transfer these findings to the isoelectronic  $\text{C}_7\text{H}_5^+$  potential energy surface (PES) by formally replacing the BH group by the  $\text{CH}^+$  unit (Fig. 1) [17–19].

## 2. Experimental

We conducted the experiments under single collision conditions utilizing a crossed molecular beams machine [20]. Briefly, a pulsed boron atom beam,  $\text{B}(^2\text{P}_j)$ , was generated in the primary source via laser ablation of a boron rod at 266 nm (30 Hz). The ablated species were seeded in neat carrier gas (helium, 99.9999%, Airgas; 4 atm; Table 1) released by a Proch–Trickl pulsed valve. After passing a skimmer, a four-slot chopper wheel selected a part of the pulsed boron beam which then crossed a pulsed, argon seeded (740 Torr) benzene or D6-benzene beam ( $\text{C}_6\text{H}_6$ ; Aldrich, 99.9%;  $\text{C}_6\text{D}_6$ ; Aldrich, 99+%); seeding fractions of about 5% benzene/D6-benzene were obtained. We observed the reactively scattered species using a triply differentially pumped quadrupole mass spectrometric detector (QMS) in the time-of-flight (TOF) mode after electron-impact ionization of the neutral molecules. The detector was rotatable within the plane defined by the primary and the secondary reactant beams; this allowed taking angular resolved TOF spectra. By integrating the TOF spectra, we obtained the laboratory angular distribution (LAB). Information on the chemical dynamics were gathered by fitting the TOF spectra and the LAB distributions using a forward-convolution routine [21,22]. Best fits of the TOF and laboratory angular distributions were

Table 1  
Peak velocities ( $v_p$ ), speed ratios ( $S$ ) and center-of-mass angles ( $\theta_{\text{CM}}$ ) together with the nominal collision energies of the boron and the benzene reactants ( $E_c$ )

Beam	$v_p$ ( $\text{ms}^{-1}$ )	$S$	$E_c$ ( $\text{kJ mol}^{-1}$ )	$\theta_{\text{CM}}$
$\text{C}_6\text{H}_6(\text{X}^1\text{A}_{1g})/\text{Ar}$	$640 \pm 10$	$15.7 \pm 1.0$		
$\text{B}(^2\text{P}_j)/\text{He}$	$2160 \pm 8$	$3.5 \pm 0.1$	$24.5 \pm 0.2$	$64.5 \pm 0.2$
$\text{C}_6\text{D}_6(\text{X}^1\text{A}_{1g})/\text{Ar}$	$630 \pm 10$	$15.7 \pm 1.0$		
$\text{B}(^2\text{P}_j)/\text{He}$	$2170 \pm 8$	$3.5 \pm 0.1$	$24.8 \pm 0.2$	$65.7 \pm 0.2$

achieved by refining the adjustable  $T(\theta)$  and  $P(E_T)$  parameters.

## 3. Results

Reactive scattering signal was observed at mass-to-charge ratios,  $m/z$ , of 88 ( $^{11}\text{BC}_6\text{H}_5^+$ ), 87 ( $^{10}\text{BC}_6\text{H}_5^+ / ^{11}\text{BC}_6\text{H}_4^+$ ), and 86 ( $^{10}\text{BC}_6\text{H}_4^+ / ^{11}\text{BC}_6\text{H}_3^+$ ) [benzene reactant] and at  $m/z = 93$  ( $^{11}\text{BC}_6\text{D}_5^+$ ), 91 ( $^{11}\text{BC}_6\text{D}_4^+$ ), and 89 ( $^{11}\text{BC}_6\text{D}_3^+$ ) [D6-benzene reactant] (Fig. 2). For both the benzene and D6-benzene systems, TOF spectra at all mass-to-charge ratios were found to be superimposable. Therefore, signal from lower  $m/z$  values originates from isotopomers and/or dissociative ionization of the  $^{11}\text{BC}_6\text{H}_5$  and  $^{11}\text{BC}_6\text{D}_5$  parent molecules in the electron-impact ionizer. Also, our findings suggest that the atomic boron versus atomic hydrogen (deuterium) pathway is open; the molecular hydrogen and deuterium elimination channels are closed. These TOF data can now be integrated and scaled to extract the laboratory angular distributions of the  $^{11}\text{BC}_6\text{H}_5$  and  $^{11}\text{BC}_6\text{D}_5$  products (Fig. 2). Here, the LAB distributions peak at  $64^\circ$  and  $65.5^\circ$  close to the center-of-mass angles of  $64.5^\circ$  and  $65.7^\circ$  for benzene and D6-benzene, respectively. In addition, the narrow ranges of the LAB distributions of about  $30^\circ$  suggest that the averaged translational-energy releases are relatively small. Most importantly, for deuterated benzene, signal was also observed at  $m/z = 95$ , i.e.  $^{11}\text{BC}_6\text{D}_6^+$  (Fig. 3). The existence of an adduct – which has also been observed in the related reactions of ground-state oxygen ( $\text{O}(^3\text{P}_j)$ ) [23] and carbon atoms ( $\text{C}(^3\text{P}_j)$ ) [24] with benzene – proves unassailably that this reaction proceeds via an indirect reaction mechanism. It should be stressed that the intensity of signal of the adduct at  $m/z = 95$  was a factor of about 50 weaker than the signal at  $m/z = 93$ ; also, the adduct could be monitored only at the center-of-mass angle of  $65.5^\circ$ . No signal was found at  $63^\circ$  and at  $67^\circ$ . This is not surprising. In the related reaction of carbon atoms with benzene, the formation of the adduct could also be verified. Here, the adduct was spread over an angular range of only  $5^\circ$ . However, the signal of the  $\text{C}_7\text{D}_6^+$  adduct was stronger by a factor of 5 compared to the  $^{11}\text{BC}_6\text{D}_6^+$  adduct. Based on the signal-to-noise ratio of signal at  $m/z = 95$ , we would not expect to see any  $^{11}\text{BC}_6\text{D}_6^+$  at laboratory angles larger or smaller than the center-of-mass angle.

The translational energy distributions in the center-of-mass frame,  $P(E_T)$ s, are depicted in Fig. 4. As evident from the patterns, both  $P(E_T)$ s are very similar and were fitted with similar parameters with less than 6% change due to the mass differences of the reactants and product molecules. Best fits of the laboratory could be achieved with a single  $P(E_T)$  for each system extending to maximum translational energy releases ( $E_{\text{max}}$ ) of about  $80\text{--}95 \text{ kJ mol}^{-1}$ . Note that  $E_{\text{max}}$  presents the sum of the reaction exoergicity and the collision energy. Therefore, by subtracting the collision energy from the high-energy cutoff, we are left with experimental exoergicities of about  $63 \pm 8 \text{ kJ mol}^{-1}$ . This

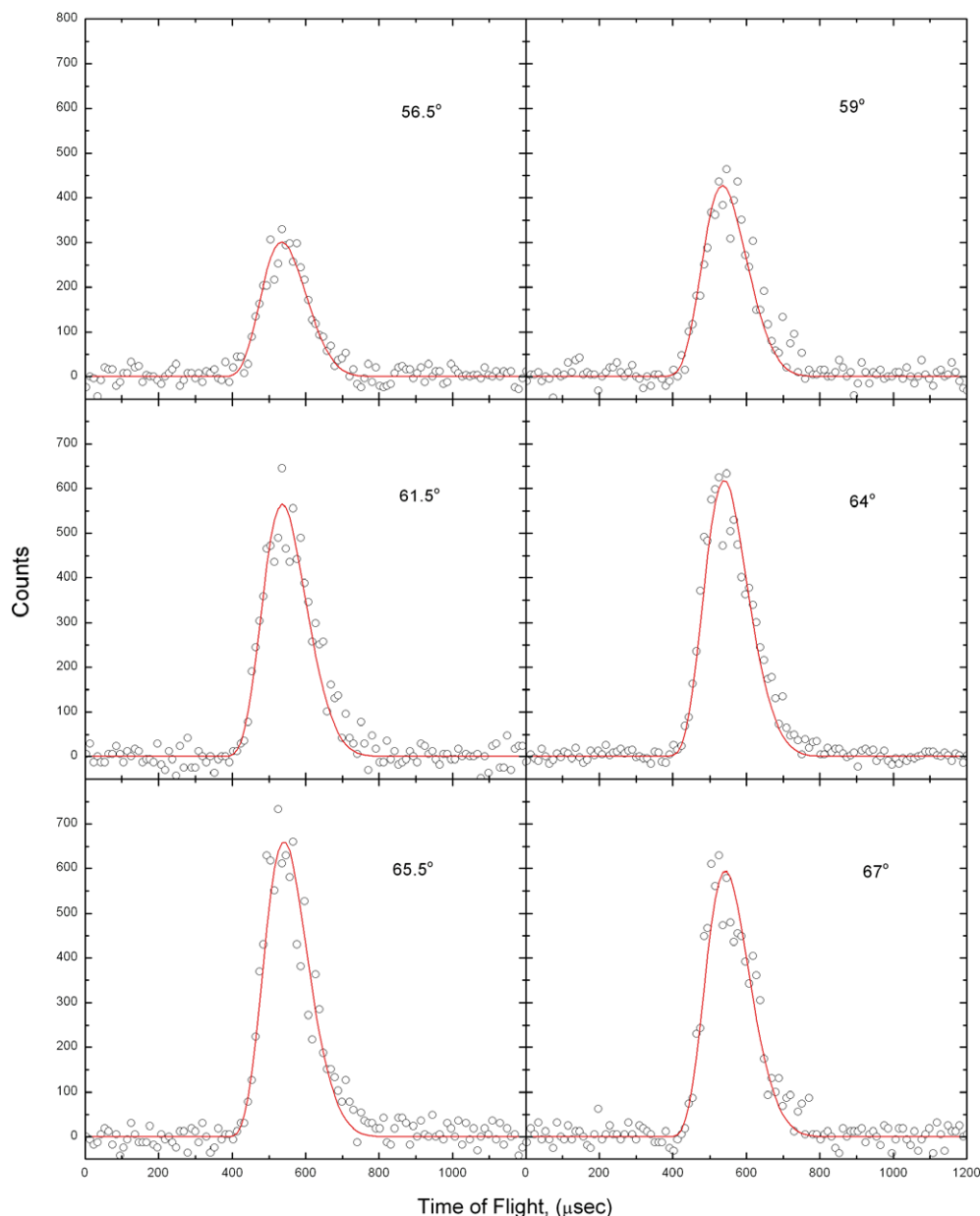


Fig. 2a. Time-of-flight data at  $m/z = 88$  ( $^{11}\text{BC}_6\text{H}_5^+$ ) recorded for the reaction  $^{11}\text{B}(^2\text{P}_j)$  with  $\text{C}_6\text{H}_6(\text{X}^1\text{A}_{1g})$  at various laboratory angles at a collision energy of  $24.5 \text{ kJ mol}^{-1}$ . The circles represent the experimental data, and the solid line represents the fit. Each TOF spectrum has been normalized to the relative intensity of each angle.

experimental data can later be compared to *ab initio* calculations to identify the nature of the product isomer(s). We would like to stress that the fits were found to be very sensitive to the peak position. The  $P(E_T)$  peak away from zero translational energy and show a plateau between 15 and  $20 \text{ kJ mol}^{-1}$ . This finding indicates the presence of an exit barrier and a tight exit transition state.

The center-of-mass angular distributions,  $T(\theta)$ s, also give valuable information on the reaction mechanism (Fig. 4). Both distributions show intensity over the complete angular range and are symmetric around  $90^\circ$ . This feature implies that the lifetime of the decomposing complex(es) is(are) longer than the rotational period. Also,

both center-of-mass angular distributions show maxima at  $90^\circ$ . Ratios of the flux intensities at  $0^\circ$  versus  $90^\circ$  are  $1.3 \pm 0.1$  and  $1.6 \pm 0.1$  for the benzene and D6-nbenzene reactants, respectively. The maxima at  $90^\circ$  strongly suggest geometrical constraints of the decomposing complex, here, a preferential H(D) atom ejection perpendicular to the molecular plane of the  $^{11}\text{BC}_6\text{H}_5/^{11}\text{BC}_6\text{D}_5$  moieties almost parallel to the total angular momentum vector [16].

#### 4. Discussion

The first step in finding the actual reaction mechanism is to identify the reaction product(s). For this, we contrast the

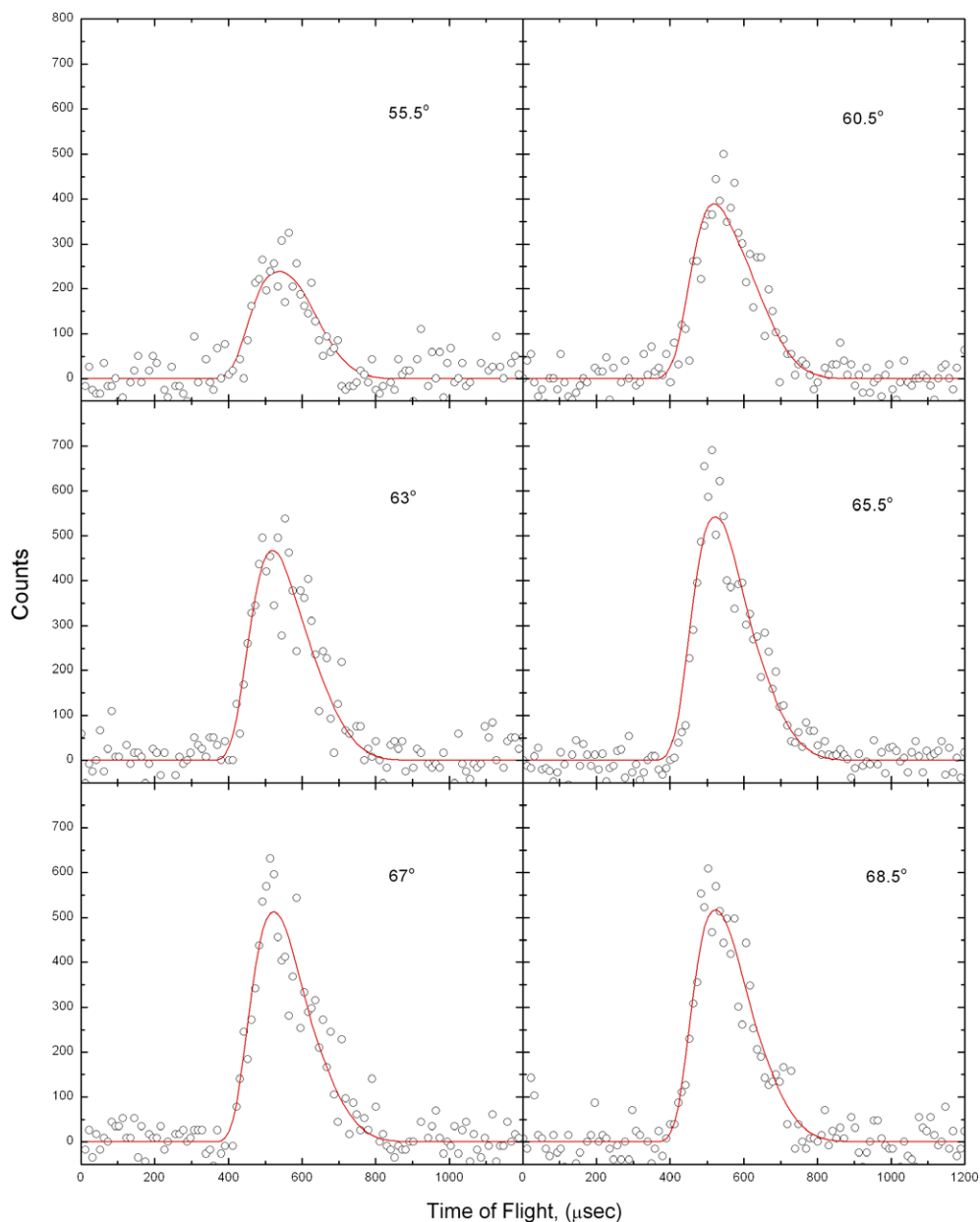


Fig. 2b. Time-of-flight data at  $m/z = 93$  ( $^{11}\text{BC}_6\text{D}_5^+$ ) recorded for the reaction  $^{11}\text{B}(^2\text{P}_j)$  with  $\text{C}_6\text{D}_6(\text{X}^1\text{A}_{1g})$  at various laboratory angles at a collision energy of  $24.8 \text{ kJ mol}^{-1}$ . The circles represent the experimental data, and the solid line represents the fit. Each TOF spectrum has been normalized to the relative intensity of each angle.

experimentally determined reaction energy with those for different isomers determined from *ab initio* calculations. The translational energy distributions show that the formation of the  $^{11}\text{BC}_6\text{H}_5/^{11}\text{BC}_6\text{D}_5$  isomer(s) is exoergic by  $63 \pm 8 \text{ kJ mol}^{-1}$ . Previous electronic structure calculations located three  $^{11}\text{BC}_6\text{H}_5/^{11}\text{BC}_6\text{D}_5$  isomers, **p1**–**p3** (Fig. 5). Only the reaction to form **p1** was found to be exoergic by  $70 \pm 10 \text{ kJ mol}^{-1}$  ( $^{11}\text{BC}_6\text{D}_5$ ) [15] and  $80 \pm 10 \text{ kJ mol}^{-1}$  ( $^{11}\text{BC}_6\text{H}_5$ ) [16]. These data match well with our experimental findings. The reactions to synthesize **p2/p3** + H were found to be endoergic by about 62 and  $106 \text{ kJ mol}^{-1}$ , respectively. Considering the collision energies in our experiments (Table 1), these data make the for-

mation of **p2/p3** energetically not feasible. Consequently, it is obvious that **p1** is the only likely reaction product formed via an  $^{11}\text{B}$  versus atomic hydrogen/deuterium exchange pathway. Based on these energetics and the translational energy distributions, we can compute the fraction of energy channeling into the translational motion of the products to be  $33 \pm 3\%$ . This order of magnitude suggests also the presence of indirect scattering dynamics. Also, we would like to recall that the  $P(E_T)$ s suggested the existence of an exit barrier once the  $^{11}\text{BC}_6\text{H}_6/^{11}\text{BC}_6\text{D}_6$  intermediates decompose to **p1** + H/D. Since **p1** presents an unsaturated closed-shell product (as a matter of fact **p1** is an aromatic molecule) [16], the principle of microscopic reversibility of an

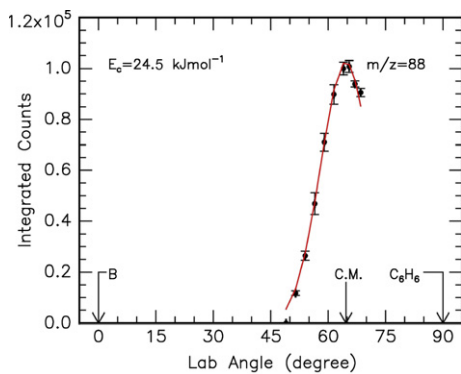


Fig. 2c. Lower: Newton diagram for the reaction  $^{11}\text{B}(^2\text{P}_j) + \text{C}_6\text{H}_6(\text{X}^1\text{A}_{1g})$  at a collision energy of  $24.5 \text{ kJ mol}^{-1}$ . Upper: Laboratory angular distribution of the  $^{11}\text{BC}_6\text{H}_5$  product at  $m/z = 88$ . Circles and  $1\sigma$  error bars indicate experimental data, the solid line the calculated distribution. The solid lines originating in the Newton diagram point to distinct laboratory angles whose times of flight are shown in Fig. 2a.

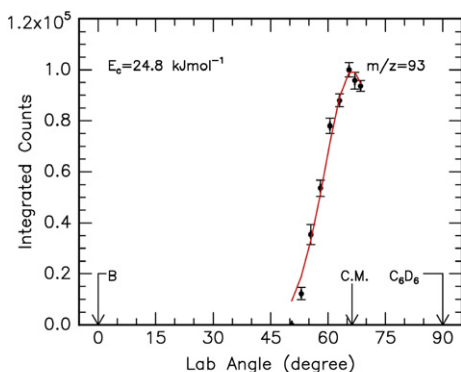


Fig. 2d. Lower: Newton diagram for the reaction  $^{11}\text{B}(^2\text{P}_j) + \text{C}_6\text{D}_6(\text{X}^1\text{A}_{1g})$  at a collision energy of  $24.8 \text{ kJ mol}^{-1}$ . Upper: Laboratory angular distribution of the  $^{11}\text{BC}_6\text{D}_5$  product at  $m/z = 93$ . Circles and  $1\sigma$  error bars indicate experimental data, the solid line the calculated distribution. The solid lines originating in the Newton diagram point to distinct laboratory angles whose times of flight are shown in Fig. 2b.

addition of a hydrogen/deuterium atom to a closed shell aromatic system dictates that this reverse process should have an entrance barrier. The experimentally derived peak-

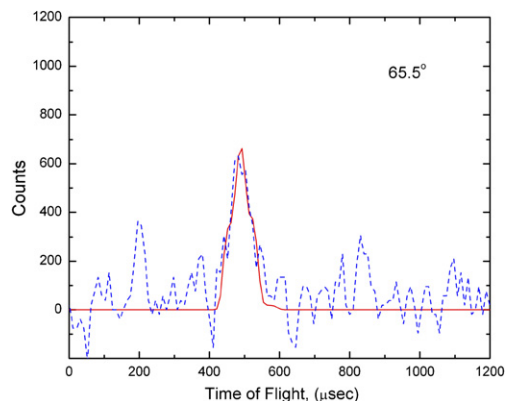


Fig. 3. Time-of-spectrum of the  $^{11}\text{BC}_6\text{D}_6$  adduct recorded at  $m/z = 95$  at a laboratory angle of  $65.5^\circ$ . In the fitting routine, the lab data (dashed line) has been fitted (solid line) with a mass combination of  $94.999 \text{ amu}$  and  $0.001 \text{ amu}$ ; the translational energy distribution peaked at zero translational energy and extended to a few  $\text{kJ mol}^{-1}$ .

ing of the  $P(E_T)$ s of  $15\text{--}20 \text{ kJ mol}^{-1}$  is similar to the entrance barrier found in the addition of a hydrogen atom to benzene, i.e.  $37 \text{ kJ mol}^{-1}$  [25].

Having established the formation of the benzoborirene molecule, **p1**, we attempt now to solve the underlying reaction dynamics to form this isomer on the doublet  $^{11}\text{BC}_6\text{D}_6$  and  $^{11}\text{BC}_6\text{H}_6$  surfaces. First, the detection of the  $^{11}\text{BC}_6\text{D}_6$  adduct in the boron – D6-benzene system and the shapes of the center-of-mass angular distributions clearly indicate that the reactions of atomic boron with benzene and D6-benzene are indirect and proceed through a long-lived intermediate via a boron addition – hydrogen/deuterium atom elimination pathway. As expected from reactions of electron deficient boron atoms with unsaturated hydrocarbons [14,26–29], the intermediate results from the addition of a boron atom to the benzene ring. In principle, three initial addition products exist (Fig. 5): addition to the corner of the benzene molecule (**i1**), to the edge of the benzene molecule involving the C1 and C2 positions (**i2**), and across the benzene ring adding to C1 and C4 (**i3**). Theoretical calculations show that **i2** is not a local minimum but a transition state for a boron migration across the benzene ring, for example a migration from the C1 atom in **i1** to C2 [16]. Likewise, the transannular intermediate **i3** must be classified as a transition state. Here, the boron atom in the initial  $\text{C}_{2v}$  symmetric intermediate can be tilted toward one of the carbon–carbon double bonds thus effectively reducing the symmetry to  $\text{C}_s$ . However, this process involved second order stationary points. Consequently, no low-lying path exists in the relaxation from  $\text{C}_{2v}$  to  $\text{C}_s$  symmetry. Therefore, among three feasible addition complexes, only the initial adduct **i1** turns out to be a local minimum. The isomerization of **i1** ultimately lead to the phenylboranyl radical **i6** and does not involve barriers higher than the energy of the separated reactants. Phenylboranyl was found to decompose via cleavage of an *ortho*-carbon–hydrogen bond and concomitant ring-closure to yield ultimately the benzoborirene product via a tight exit tran-

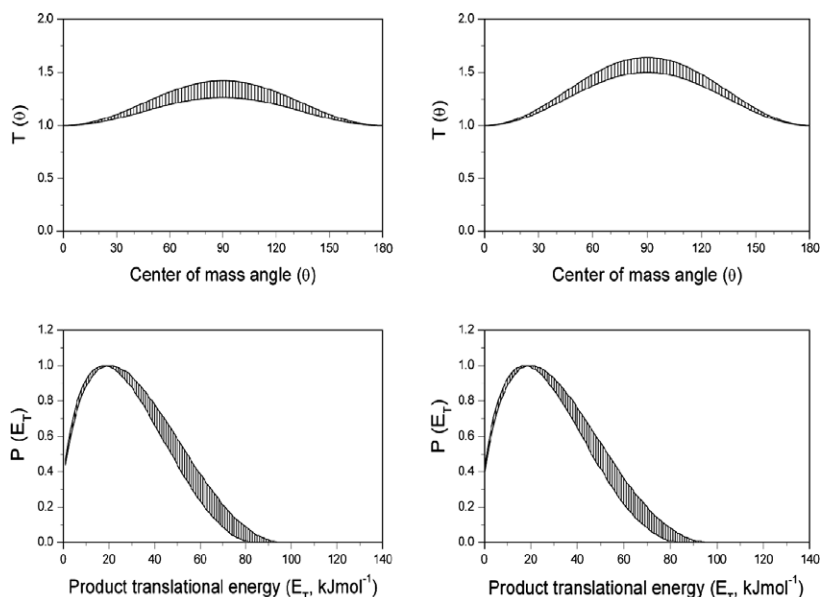


Fig. 4. Center-of-mass angular (upper) and translational energy (lower) distributions for the reactions of  $^{11}\text{B}(^2\text{P}_j) + \text{C}_6\text{H}_6(\text{X}^1\text{A}_{1g})$  and  $^{11}\text{B}(^2\text{P}_j) + \text{C}_6\text{D}_6(\text{X}^1\text{A}_{1g})$  to form  $^{11}\text{BC}_6\text{H}_5 + \text{H}$  (left column) and  $^{11}\text{BC}_6\text{D}_5 + \text{D}$  (right column).

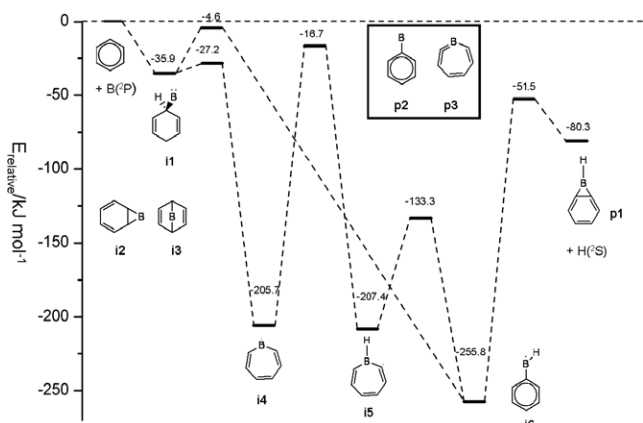


Fig. 5. Schematic potential energy surface of the reaction of  $^{11}\text{B}(^2\text{P}_j)$  plus  $\text{C}_6\text{H}_6(\text{X}^1\text{A}_{1g})$  to form  $^{11}\text{BC}_6\text{H}_5 + \text{H}$ . Data are extracted from Ref. [16]. Also shown are the structures of the two remaining, stable  $^{11}\text{BC}_6\text{H}_5$  isomers **p2** and **p3**.

sition state located about  $29 \text{ kJ mol}^{-1}$  above the products. The existence of this exit barrier is well supported by our experimental data, i.e. a peaking of the center-of-mass translational energy distributions at  $15\text{--}20 \text{ kJ mol}^{-1}$ . Also, the center-of-mass angular distributions verify the computed geometry of the exit transition state.<sup>16</sup> Recall that the distributions peak at  $90^\circ$ , which is indicative of a reversed addition of a hydrogen/deuterium atom perpendicularly to the molecular plane of the  $^{11}\text{BC}_6\text{H}_5$ / $^{11}\text{BC}_6\text{D}_5$  benzenoborirene molecules. Here, the hydrogen/deuterium atom adds to the  $\pi$ -electron density of the aromatic benzenoborirene species at the bridge-carbon atom perpendicularly to the molecular plane. This approach geometry leads to the largest orbital overlap and hence presents the lowest energy pathway via addition.

Finally, we would like to comment briefly on the polarization of the center-of-mass angular distributions. It is well established that when a long-lived complex is formed during a reaction,  $T(\theta)$  is characterized by forward-backward symmetry, i.e. the angular distribution is symmetric with respect to  $\theta = 90^\circ$  [30]. The shape of the  $T(\theta)$  is determined by the disposal of the total angular momentum  $\mathbf{J}$  and a variety of shapes are indeed possible. In crossed beam experiments, the reactant molecules undergo a supersonic expansion and a substantial rotational cooling occurs; therefore, the total angular momentum is mainly given by the initial orbital angular momentum  $\mathbf{L}$ . The products can be rotationally excited, however, so that Eq. (1) is valid:

$$\mathbf{J} \approx \mathbf{L} \approx \mathbf{L}' + \mathbf{j}' \quad (1)$$

with the rotational angular momenta of the products  $\mathbf{j}'$ , and the initial and final orbital angular momenta  $\mathbf{L}$  and  $\mathbf{L}'$ . The final recoil velocity vector,  $\mathbf{v}'$ , is in a plane perpendicular to  $\mathbf{L}'$  and therefore, when the rotational excitation of products is significant,  $\mathbf{v}'$  is not in a plane perpendicular to  $\mathbf{J}$ . When  $\mathbf{j}'$  is not zero, the probability distribution for the scattering angle  $\theta$ , which is the center-of-mass angle between the initial relative velocity  $\mathbf{v}$  and  $\mathbf{v}'$ , depends on the values of  $J$ ,  $M$  and  $M'$  where  $M$  and  $M'$  are the projections of  $\mathbf{J}$  on the initial and final relative velocity, respectively. For instance, if the complex dissociates preferentially with low  $M'$  values, the final velocity  $\mathbf{v}'$  is almost perpendicular to  $\mathbf{J}$  and therefore  $\mathbf{v}'$  and  $\mathbf{v}$  are almost parallel; in this case, the product intensity will be mainly confined to the poles,  $\theta = 0^\circ$  and  $\theta = 180^\circ$ , similarly to the case of no product rotational excitation. On the contrary, when the collision complex dissociates mainly with high  $M'$  values, the final relative velocity will be almost parallel to  $\mathbf{J}$  and

perpendicular to  $\mathbf{v}$  and the products will be preferentially scattered at  $\theta = 90^\circ$ . Usually, a distribution of  $M'$  values is possible; in some cases, however, the geometry of the decomposing complex may imply a most probable  $M'$  value.

In the present systems, the  $T(\theta)$ s exhibit a symmetric shape and a peaking at  $\theta = 90^\circ$  suggesting that the H(D) atom is ejected more favorably in a direction close to the direction of the total angular momentum. As a matter of fact, the  $T(\theta)$  derived in the boron-D6-benzene system is slightly stronger polarized than the distribution found in the boron–benzene experiment. Since the final orbital angular momentum  $\mathbf{L}'$  is simply the product of the impact parameter, the relative velocity of the departing products, and the reduced mass of the products, we expect that due to the heavier mass of the deuterium atom, the final orbital angular momentum in the boron-D6-benzene system is larger than in the boron–benzene case. Therefore,  $\mathbf{L}$  and  $\mathbf{L}'$  are expected to be stronger coupled in the boron-D6-benzene system which in turn is reflected in the enhanced polarization of the corresponding  $T(\theta)$ .

Here, we would also like to discuss the isoelectronic benzocyclopropyl cation (Fig. 1) in the light of our experimental findings. As early as 1930, Miller and Nixon found that a fused small ring exerted a decisive influence on the directional selectivity of the benzene nucleus in electrophilic substitution reactions [31]. In a more recent paper, *ab initio* calculation of geometric and bonding features of this cation show a substantial aromatic character of the fused three-membered ring; the computations suggested that two antagonistic  $\pi$ -electron distribution patterns determine the electrophilic reactivity [32]. Jursic compared the isodesmic energies and HOMO–LUMO gaps of the benzyl with the benzocyclopropyl cation; the results showed that a ring closure to a bicyclic structure produces a more stable (aromatic) system [33]. Experimentally, Smith et al studied the mechanism of singly ionized carbon atoms,  $\text{C}^+(^2\text{P})$ , with benzene at collision energies of 96–1150  $\text{kJ mol}^{-1}$  [34]. They found the benzene molecular ion was the principal product at all collision energies; the  $\text{C}_7\text{H}_5^+$  ion was not considered [34]. However, a  $\text{C}_7\text{H}_5^+$  ion of an unknown structure was detected as one of the primary dissociative recombination products of benzene ( $\text{C}_6\text{H}_6$ ) and singly ionized carbon cations by Abouelaziz et al. [35]. However, based on our experimental findings we can suggest that the reaction of singly ionized carbon atom with benzene produces the benzocyclopropyl cation.

## 5. Conclusions

The reactions of ground-state boron atoms,  $\text{B}(^2\text{P}_j)$ , with benzene,  $\text{C}_6\text{H}_6(\text{X}^1\text{A}_{1g})$ , and deuterated benzene  $\text{C}_6\text{D}_6(\text{X}^1\text{A}_{1g})$ , were studied at a collision energies of 24.5 and 24.8  $\text{kJ mol}^{-1}$  using the crossed molecular beam technique. It was found that the reaction follows indirect scattering reaction dynamics proceeding via an experimentally detected  $^{11}\text{BC}_6\text{D}_6$  adduct. The data suggest that the reaction proceeds via addition of the boron atom to one carbon

atom of the benzene ring following unimolecular isomerization to the phenylboryl radical intermediate,  $\text{C}_6\text{H}_5\text{BH}/\text{C}_6\text{D}_5\text{BD}$ . The latter decomposed via a tight exit transition state by cleavage of the *ortho*-carbon–hydrogen bond and concomitant ring closure to form the thermodynamically most stable  $\text{C}_6\text{H}_5\text{B}/\text{C}_6\text{D}_5\text{B}$  isomer, i.e. benzoborirene (**p1**), plus atomic hydrogen/ deuterium. Our experiments provide further a clean pathway to synthesize the benzoborirene molecule under single collision conditions and could pave the way to further spectroscopic studies of this important reaction intermediate.

## Acknowledgement

This work was supported by the Air Force Office of Scientific Research (AFOSR; W911NF-05-1-0448). The authors thank Ed Kawamura (University of Hawaii, Department of Chemistry) for his electrical work.

## References

- [1] H.W. Jin, Q.S. Li, PCCP 5 (2003) 1110.
- [2] K.C. Schadow, K.J. Wilson, E. Gutmark, R.A. Smith, *Combust. Boron-Based Solid Propellants Solid Fuels* (1993) 402.
- [3] E.L. Dreizin, D.G. Keil, W. Felder, E.P. Vicenzi, *Combust. Flame* 119 (1999) 272.
- [4] S. Williams et al., *CPIA Publ.* 703 (2000) 205.
- [5] O. Novotny, B. Sivaraman, C. Rebrion-Rowe, D. Travers, L. Biennier, J.B.A. Mitchell, B.R. Rowe, *J. Chem. Phys.* 123 (2005) 104303/1.
- [6] A.M. Savel'ev, A.M. Starik, *Tech. Phys.* 51 (2006) 444.
- [7] I.M.E. Volpin, Y.D. Koreshkov, V.G. Dulova, D.N. Kursanov, *Tetrahedron* 18 (1962) 107.
- [8] C.U. Pittman Jr., L.D. Kispert, T.B. Patterson Jr., *J. Phys. Chem.* 77 (1973) 494.
- [9] Y.G. Byun, S. Saebø, C.U. Pittman Jr., *J. Am. Chem. Soc.* 113 (1991) 3689.
- [10] J.J. Eisch, K. Tamao, R.J. Wilcsek, *J. Am. Chem. Soc.* 97 (1975) 895.
- [11] J.J. Eisch, B. Shafii, A.L. Rheingold, *J. Am. Chem. Soc.* 109 (1987) 2526.
- [12] D.V. Lanzisera, P. Hassanzadeh, Y. Hannachi, L. Andrews, *J. Am. Chem. Soc.* 119 (1997) 12402.
- [13] L. Andrews, D.V. Lanzisera, P. Hassanzadeh, Y. Hannachi, *J. Phys. Chem. A* 102 (1998) 3259.
- [14] N. Balucani, O. Asvany, Y.T. Lee, R.I. Kaiser, N. Galland, Y. Hannachi, *J. Am. Chem. Soc.* 122 (2000) 11234.
- [15] R.I. Kaiser, H.F. Bettinger, *Angewandte Chemie, Int. Ed.* 41 (2002) 2350.
- [16] H.F. Bettinger, R.I. Kaiser, *J. Phys. Chem. A* 108 (2004) 4576.
- [17] B. Halton, M.P. Halton, *Tetrahedron* 29 (1973) 1717.
- [18] O. Sinanoglu, *Tetrahedron Lett.* 29 (1988) 889.
- [19] A. Stanger, *J. Am. Chem. Soc.* 120 (1998) 12034.
- [20] X. Gu, Y. Guo, E. Kawamura, R.I. Kaiser, *J. Vac. Sci. Technol. A* 24 (2006) 505.
- [21] M. Vernon, Ph.D., University of California, Berkeley, CA, 1981.
- [22] M.S. Weiss, Ph.D., University of California, Berkeley, CA, 1986.
- [23] S.J. Sibener, R.J. Buss, P. Casavecchia, T. Hirooka, Y.T. Lee, *J. Chem. Phys.* 72 (1980) 4341.
- [24] H.F. Bettinger, P.v.R. Schleyer, H.F. Schaefer III, P.R. Schreiner, R.I. Kaiser, Y.T. Lee, *J. Chem. Phys.* 113 (2000) 4250.
- [25] A.M. Mebel, M.C. Lin, T. Yu, K. Morokuma, *J. Phys. Chem. A* 101 (1997) 3189.
- [26] N. Balucani, O. Asvany, Y.T. Lee, R.I. Kaiser, N. Galland, M.T. Rayez, Y. Hannachi, *J. Comput. Chem.* 22 (2001) 1359.

- [27] D. Sillars, R.I. Kaiser, N. Galland, Y. Hannachi, *J. Phys. Chem. A* 107 (2003) 5149.
- [28] R.I. Kaiser, N. Balucani, N. Galland, F. Caralp, M.T. Rayez, Y. Hannachi, *PCCP* 6 (2004) 2205.
- [29] W.D. Geppert, F. Goulay, C. Naulin, M. Costes, A. Canosa, S.D. Le Picard, B.R. Rowe, *PCCP* 6 (2004) 566.
- [30] W.B. Miller, S.A. Safron, D.R. Herschbach, *Disc. Faraday Soc.* (44) (1967) 108.
- [31] W.H. Mills, I.G. Nixon, *J. Chem. Soc.* (1930) 2510.
- [32] M. Eckert-Maksic, Z. Glasovac, Z.B. Maksic, I. Zrinski, *Theochem* 366 (1996) 173.
- [33] B.S. Jursic, *Theochem* 468 (1999) 171.
- [34] R.D. Smith, J.J. DeCorpo, *J. Phys. Chem.* 80 (1976) 2904.
- [35] H. Abouelaziz, J.C. Gomet, D. Pasquero, B.R. Rowe, J.B.A. Mitchell, *J. Chem. Phys.* 99 (1993) 237.